MULTIFUNCTIONAL (NO_x/CO/O_2) SOLID-STATE SENSORS FOR COAL COMBUSTION CONTROL

Technical Progress Report

Start Date: September 30, 2003
End Date: October 1, 2004

Eric D. Wachsman

March 21, 2005

DOE Award Number – DE-FG26-02NT41533

Department of Materials Science and Engineering
University of Florida
Gainesville, FL 32611-6400

DISCLAIMER

ABSTRACT

Sensing properties of a La_2CuO_4- and WO_3-based potentiometric NO_x sensor were investigated both in N_2 and in a simulated exhaust gas. We performed temperature programmed reaction (TPR) and desorption (TPD) experiments to determine the reaction and adsorption characteristics of O_2, NO_x, CO, CO_2, and their mixtures on the electrodes, and related the results to sensor performance.

The relative responses of the La_2CuO_4-based sensor under varied concentrations of NO, NO_2, CO, CO_2 and O_2 were studied. The results showed a very high sensitivity to CO and NO_2 at 450 ºC in 3 % O_2, whereas the response to O_2 and CO_2 gases was negligible. The NO response at 400 – 500 ºC agreed with the NO adsorption behavior. The high NO_2 sensitivity at 450 ºC was probably related to heterogeneous catalytic activity of La_2CuO_4. The adsorption of NO was not affected by the change of O_2 concentration and thus the sensor showed selective detection of NO over O_2. However, the NO sensitivity was strongly influenced by the existence of CO, H_2O, NO_2, and CO_2, as the adsorption behavior of NO was influenced by these gases.

The WO_3-based sensor was able to selectively detect NO in the presence of CO_2 in 3 % O_2 and at 650 ºC. The NO sensitivity, however, was affected by the variation of the NO_2, CO, and H_2O concentration. No gas-solid reactions were observed using TPR in the NO-containing gas mixture, indicating that the NO response was not obtained by the conventionally accepted mixed-potential mechanism. At the same condition the sensor had high sensitivity to ~ 10 ppm NO_2 and selectivity in the presence of CO, CO_2, and H_2O, showing it to be applicable to the monitoring of NO_2. Significantly different sensing properties of NO in simulated exhaust gas suggested the occurrence of gas composition change by the gas-phase and gas-solid reactions, and strong adsorption of water on the electrodes. The NO_2 sensitivity in simulated exhaust gas was modified by O_2 and H_2O, but not by CO and CO_2.

A positive voltage response was obtained for NO_2 but negative for NO at 650 ºC with the n-type semiconducting WO_3-based sensor. In contrast the opposite response direction for NO_x was observed at 450 ºC with the La_2CuO_4 (p-type semiconductor).

TABLE OF CONTENTS

1. INTRODUCTION

There is a tremendous environmental and regulatory need for the monitoring and control of NO_x emissions from coal, natural gas and oil combustion sources [1 – 4]. Solid oxide electrochemical O_2 sensors are inexpensive and have been well demonstrated in harsh high-temperature combustion exhaust environment. If modified to selectively measure NO_x and CO concentrations this type of sensor can be used to further improve combustion control, resulting in improved fuel utilization and reduced emissions.

We have developed solid-state sensor technology that can provide an inexpensive, rugged, small, solid-state device capable of measuring the concentration of multiple species (such as NO, NO_2 and CO) in coal, natural gas and oil combustion exhaust [5]. Our sensor technology is similar to that used in conventional automotive O_2 sensors and thus can be used directly in high temperature exhaust. However, both the sensing and reference electrode are in the same gas stream, significantly reducing fabrication costs. These small (<1 cm^2) simple potentiometric (voltage output) sensors are sensitive to each of these gasses and can be readily combined on a single chip to provide a multifunctional (NO_x, CO, O_2) sensor (Fig. 1). This technology is the basis for a low cost, simplified way to meet emissions monitoring regulations as well as to improve combustion control, thus, improving fuel utilization and reducing emissions from coal, natural gas and oil combustion sources.

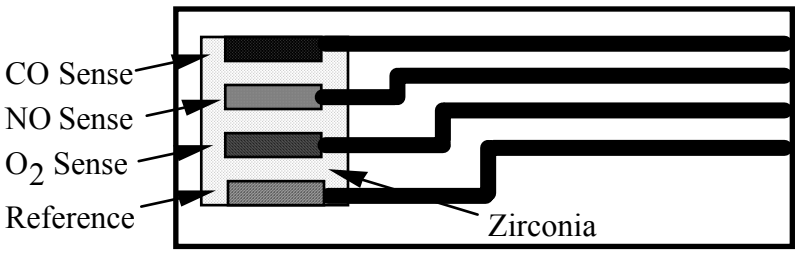

Fig. 1. Multifunctional NO_x, CO, O_2 sensor.

The key scientific issue that must be addressed for this type of sensor to effectively measure NO_x and CO concentrations in coal, natural gas and oil combustion exhaust gas streams is the selectivity of the electrode(s) for discrimination between gaseous NO_x and CO vs. O_2. Specifically, the sensors must exhibit a highly selective response to ppm levels of NO_x and CO in the presence of percent levels of O_2. Not only must the sensor exhibit a selectivity factor of, for example, 1000:1 NO/O_2, based on the typical concentration differences between NO and O_2, but the sensor must be insensitive to large changes in the O_2 concentration associated with variations in combustion conditions.

We have developed an innovative scientific approach "Differential Electrode Equilibria" (described below), and demonstrated that this approach provides the necessary selectivity to measure for example, ppm levels of NO with high sensitivity in lean-burn (13 – 17 % O_2) exhaust gas unaffected by variations in O_2 concentration. Since we have already demonstrated this works for NO, the objectives of our proposed research are to: advance the fundamental understanding of this approach, apply it to the development of selective NO_2, CO and O_2 electrode elements; fabricate and test a multifunctional (NO_x, CO, O_2) sensor; and develop a miniature low-cost multifunctional (NO_x, CO, O_2) sensor prototype for evaluation by commercial/industrial companies. In achieving these objectives we will both advance the science of solid-state electrochemical sensors, including the education and training of students, and bring closer to commercialization a device that will result in both improved fuel utilization and reduced emissions from coal, natural gas and oil combustion.

Differential Electrode Equilibria

A difference in electrochemical potential between two electrodes exposed to the same environment will occur if one or both of the electrodes does not achieve thermodynamic equilibrium. In a potentiometric sensor this non-Nernstian response produces a voltage that depends on the concentration of one or more of the species present.

Semiconducting resistive sensors have been investigated for many years for detection of gases [6]. Sensor characteristics depend on the microstructure of the material and

geometrical configuration of the sensor element. However, most of these sensors lack the ability to selectively detect the individual gases. For instance, it is difficult to monitor NO under varying O_2 concentration in combustion exhaust using only a resistive sensor.

Traditional potentiometric sensors operate on the principle that a voltage arises at the surface between two similar electrodes, fabricated on two opposite faces of an electrolyte material, when exposed to different environments [7]. The voltage is proportional to the log of the pO_2 difference.

In contrast, our sensors operate with two dissimilar electrodes exposed to the same environment. The differential electrode equilibria created between the gas molecules and the dissimilar sensor electrode surfaces give rise to a potential gradient between the electrodes, resulting in a voltage response [8]. Semiconducting oxide electrodes combined with platinum reference electrodes on YSZ substrates are sensitive and selective to NO with negligible response to O_2 or CO.

The composition and microstructure of the sensing electrode are the key parameters that influence the sensing mechanism, and hence key sensor performance parameters: sensitivity, selectivity and response time. During the previous reporting period we investigated the effect of microstructure and the fundamental heterogeneous gas-solid interactions of La_2CuO_4. We demonstrated that the microstructure of electrodes has a dramatic effect on both sensitivity and response time of potentiometric NO sensors. We also used the TPD technique to determine the adsorption characteristics of O_2, NO, CO, CO_2, and their mixtures, on the La_2CuO_4 electrode material and related the results to sensor performance.

Various potentiometric gas sensors based on semiconducting metal oxides have shown good sensitivity with stable response. Di Bartolomeo *et al.* reported that potentiometric planar sensors built using WO_3, $LaFeO_3$, $La_{0.8}Sr_{0.2}FeO_3$, and ZnO, where both electrodes were on the same face, showed fast and stable response to NO_2 and CO [9, 10]. Gas sensing properties of potentiometric tubular sensors based on semiconducting metal oxides such as WO_3, SnO_2, ZnO, CdO, MoO_3, In_2O_3, etc., were also investigated [11, 12]. Among the above oxides, WO_3 is of particular interest because it has been known to be sensitive to

NO_x without significant sensor signal drift. According to earlier studies, the potentiometric response to NO_x using a WO_3 electrode was fast and stable, and a linear relationship was obtained in a plot of the sensor emf vs. the logarithm of NO_x concentration [12, 13]. However, only limited information is currently available about the sensing properties of a WO_3-based potentiometric sensor. Therefore studies of its selectivity, stability, and reproducibility are required. In the previous report a potentiometric La_2CuO_4 sensor showed adequate and stable response to NO_x. The critical requirement for NO_x detection in combustion exhausts containing hydrocarbons, CO_2, H_2O, O_2, CO, and NO_x is the selectivity of the electrode. In this report, sensing properties and selectivities for the detection of low concentration NO_x (10 – 650 ppm) in N_2 and in a simulated exhaust gas by using asymmetrical potentiometric sensors based on La_2CuO_4 and WO_3 electrode are described. Additionally sensing mechanisms are discussed using temperature programmed reaction (TPR) and desorption (TPD) results.

2. EXECUTIVE SUMMARY

During this reporting period we investigated the selectivity of NO_x over O_2, CO, CO_2, and H_2O, as enhanced selectivity is a critical requirement for the applications in combustion exhausts. In the potentiometric sensor a potential difference arises between the two electrodes, due to dissimilarity in electrochemical reactions, catalytic activities, and adsorption of gases of either side. Along with the selectivity studies, the characteristics of the gas-phase and gas-solid reactions, and adsorption of O_2, NO_x, CO, CO_2, and their mixtures was studied by using the temperature programmed reaction (TPR) and desorption (TPD) techniques, and the results interpreted considering the sensing behavior.

The cross-sensitivities of the La_2CuO_4-based sensor for NO, NO_2, and CO were high, but for CO_2 and O_2 were negligible. The WO_3-based sensor responded highly to ~ 10 ppm NO_2 and selectively in the existence of CO, CO_2, and H_2O, showing it to be applicable to the monitoring of NO_2. No gas-solid reactions were observed in the NO-containing gas mixture during TPR experiments, indicating that the NO response was not obtained by the so-called mixed-potential mechanism.

The p-type La_2CuO_4–based sensor operated at 450 ºC with reasonably high NO sensitivity and fast response. An abrupt decrease in sensitivity occurred above 500 ºC and at 350 ºC the response was saturated, in good agreement with the TPD results. This indicates that NO sensing by La_2CuO_4 is likely due to the chemisorption of NO and the resulting change in Fermi level of the oxide.

The n-type semiconducting WO_3-based sensor showed optimal NO_2 sensing behavior at 650 ºC and the response decreased with temperature. This temperature effect can be explained using the NO_2 TPR results. Since a dissymmetry of the catalytic activity for NO_2 reduction between the two electrodes is temperature dependent and the difference decreases with temperature, the NO_2 response decreases with increasing temperature.

3. EXPERIMENTAL

3-1. Potentiometric NO_x Sensor

As described in the previous report and shown in Fig. 2, an asymmetrical planar sensor was built using an 8-mole % Y_2O_3-doped ZrO_2 plate (Marketech International Inc., YSZ-8Y, 20 × 10 × 0.1 mm) as a solid electrolyte, and a metal oxide (WO_3 or La_2CuO_4) and a Pt layer as electrodes.

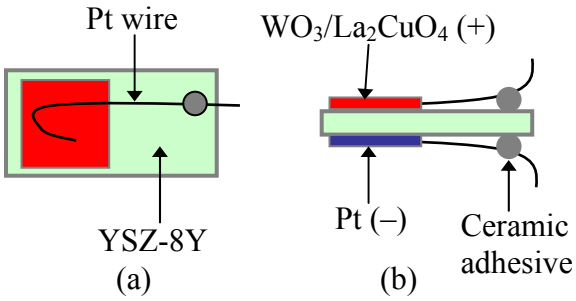

Fig. 2. Schematic diagram of a potentiometric sensor. (a) Top view, (b) Side view.

Tungsten oxide (WO_3, 99.8 % purity, Alfa Aesar) powder was purchased and La_2CuO_4 was prepared by the auto-ignition method (The details were given in the previous report). For the preparation of a sensing electrode, the powder was dispersed in ethanol with polyethylene glycol 400 (PEG-400, Avocado Research Chemicals Ltd.), and subsequently ball-milled for 24 hr. The mixed slurry was then heated at 60 ^oC for 10 hr to completely remove the ethanol. One face of the YSZ-8Y substrate was screen-printed with the WO_3 (or La_2CuO_4) slurry and the other with platinum paste (Heraeus, Conductor paste CL11-5349). Platinum wires (dia. = 0.127 mm) were connected to both electrodes. After securing the end of Pt wires with high temperature adhesive (Aremco Products Inc., Ceramabond 571-VFG-P), the sensor electrodes were sintered at 800 ^oC for 10 hr with heating and cooling rate = 1 ^oC/min. Micrographs of the sintered sensing electrodes were obtained using a scanning electron microscope (SEM, JEOL JSM 6400 SEM).

3-2. Measurements of NO_x Sensing Properties

An apparatus for the sensor measurements was constructed using a gas-tight quartz tube. The sensor was installed in the tube, where both electrodes were exposed to the same gas atmosphere, and then connected to a Keithley 2000 multimeter for the measurements of electromotive force (emf) {(–) Pt/YSZ-8Y/WO_3 (or La_2CuO_4) (+)}. A Eurotherm 2408 temperature controller was used to operate a home-made furnace. The flow rate of the gases was controlled using mass flow controllers (MFCs, MKS Instruments Inc.). The total gas flow rate was fixed at 300 cc/min. Gaseous water was produced using a water bubbler. LabView software controlled the overall experiments through GPIB and RS 232 communication ports.

The sensor was allowed to equilibrate with an initial gas environment of 3 % O_2 in N_2 or simulated exhaust gas (16 % CO_2, 100 ppm CO, 3 % O_2, and 3 % H_2O). The sensor emf was measured with increasing and then decreasing concentration steps of NO_x. The retention time at every step was 200 – 300 sec. First, the emf changes were recorded as a function of temperature, 300 – 800 ^oC, while varying the concentration of NO_x, 0 – 650 ppm. Second, the selectivities to NO_x over CO, CO_2, O_2, and H_2O were investigated both in 3 % O_2 with N_2 balance and in the simulated exhaust environment.

3-3. TPR/TPD Experiments

Gas reactions catalyzed by the WO_3 powder (W), the WO_3 film on the YSZ-8Y (W+Y), the Pt on the YSZ-8Y (Pt+Y), the YSZ substrate alone (Y), and the La_2CuO_4 powder were analyzed using the temperature-programmed reaction (TPR) technique. Additionally, the TPR experiments were performed using a blank reactor (B) to determine the uncatalyzed reaction. Initially, 500 – 2000 ppm of the reactant gases or the gas mixtures flowed at 30 cc/min through the reactor at 50 ºC. When the gas flow was stabilized, the temperature was increased from 50 to 800 ºC at 30 ºC/min while measuring the concentration of effluent gases with a quadrupole mass spectrometer (QMS). We scanned carbon fragment (m/e =

12), nitrogen fragment (m/e = 14), CO (m/e = 28), NO (m/e = 30), O_2 (m/e = 32), CO_2 (m/e = 44), N_2O (m/e = 44) and NO_2 (m/e = 46) during the TPR measurements.

The temperature-programmed desorption (TPD) experiments were performed to investigate the adsorption characteristics of exhaust gases such as NO, CO, O_2, CO_2, and their mixtures on 0.033 g La_2CuO_4 powder (total BET surface area ≈ 0.066 m^2). The TPD experiments started with the adsorption of a particular gas (or gas mixture) at 300 ºC for 30 min. The reactor was then cooled down to 30 ºC at 5 ºC/min and then purged at 30 ºC with Helium containing 1 % Argon for internal calibration. The temperature was then increased from 50 to 800 ºC under flowing 30 cc/min Helium and the desorption products measured with the QMS.

4. RESULTS AND DISCUSSION

4-1. La_2CuO_4-based Sensor

4-1-1. Sensing properties of La_2CuO_4-based sensor

The sensor emf (mV) obtained with variation of NO concentration is plotted against time (sec) in Fig. 3 (a). The NO concentration at each step is labeled in the figure.

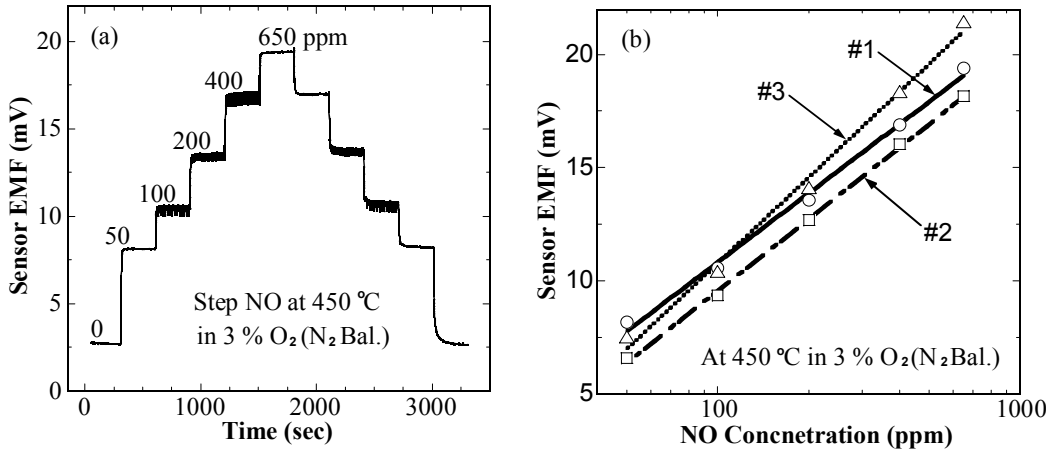

Fig. 3. Sensor response to NO concentration (0 – 650 ppm) at 450 ºC in 3 % O_2 with N_2 balance. (a) Typical plot of sensor EMF (mV) vs. NO concentration step, (b) Reproducibility of sensor EMF vs. NO concentration (ppm) for different measurements under same conditions.

The response time (t_R), time required to reach 90 % of the steady-state emf value, was less than 30 sec, irrespective of gas concentrations at 450 ºC. As shown in Fig. 3 (b), the measurement of NO showed good reproducibility between different measurements repeated over a 300 hr period under the same conditions.

The relative response with varying NO, NO_2, CO, CO_2 and O_2 concentrations are plotted in Fig. 4. Results show a high sensitivity to NO, CO, and NO_2 at 450 ºC, whereas the cross-sensitivity to O_2 and CO_2 was negligible.

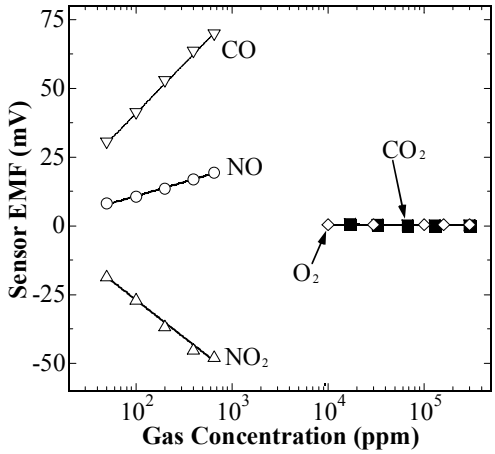

Fig. 4. La_2CuO_4 sensor response to NO, NO_2, CO, and CO_2 in 3 % O_2, and O_2 in N_2, at 450 ºC.

4-1-2. Temperature dependence of La_2CuO_4-based sensor

The temperature dependence of the NO response was investigated at $350 < T < 550$ ºC (Fig. 5 (a)).

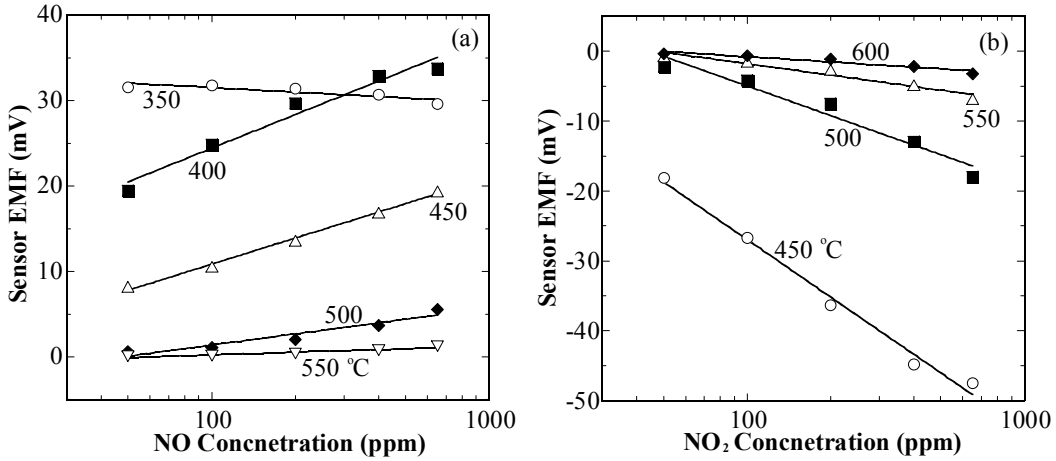

Fig. 5. Variation of the NO_x and CO sensitivity as a function of temperature in 3 % O_2. (a) NO, (b) NO_2, and (c) CO.

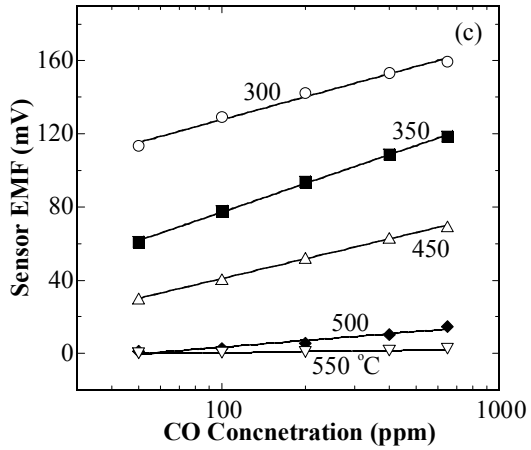

Fig. 5. (cont.) Variation of the NO_x and CO sensitivity as a function of temperature in 3 % O_2. (a) NO, (b) NO_2, and (c) CO.

Above 500 ºC values of the emf were very small, less than 5 mV for 650 ppm NO, and at 350 ºC and below the response was saturated. This temperature dependence can be explained by the TPD (Fig. 6 (a)) and TPR results. From TPR results no reaction for either direct decomposition of NO to N_2 and O_2, or oxidation of NO to NO_2 was observed up to 800 ºC. Thus any catalytic mechanism (e.g. mixed potential) can be ruled out. Therefore, the mechanism is due to adsorption of the gas and the resulting change in Fermi level of the oxide. Nitric oxide was physically and chemically adsorbed onto the oxide surface at T < 400 ºC, thus saturating the surface and sensor response at low temperature.

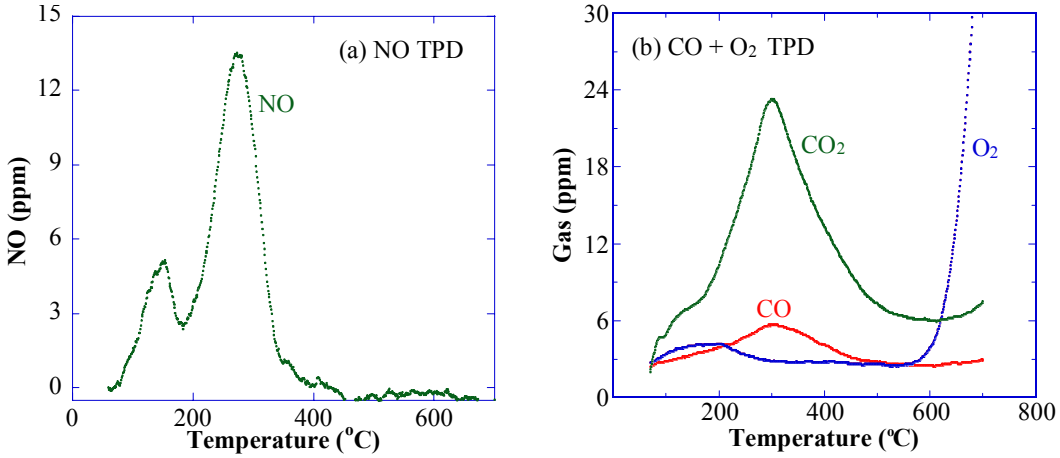

Fig. 6. TPD of (a) NO (1 %) and (b) CO (500 ppm) + O_2 (1 %) over the La_2CuO_4 powder.

The plot of the sensor emf (mV) vs. logarithm of CO concentration (ppm) is linear at 300 < T < 550 ºC (Fig. 5 (c)). The sensor was very sensitive to CO at T < 450 ºC. CO TPD results show broad desorption of CO_2 and CO at 200 < T < 450 ºC in Fig. 6 (b), indicating that the high CO response is likely due to by CO adsorption and its related surface oxidation.

Temperature dependence of the NO_2 sensitivity was also studied. As presented in Fig. 5 (b), the NO_2 response was also strongly temperature-dependent with an abrupt decrease above 500 ^oC. The TPR results (Fig. 7 (a)) show that above 250 ºC NO_2 is reduced to NO and that by 600 ºC it is completely reduced. Thus the NO_2 response at this temperature range involves heterogeneous catalysis in sensitivity. The NO_2 TPD also shows signs of surface reaction (Fig. 7 (b)). Nitrogen dioxide began desorption at 225 ^oC, and the peak was followed by a similar desorption peak for NO, shifted 25 ºC higher and the second NO desorption peak lined up with the desorption peak for chemisorbed oxygen. At temperatures above 600 ^oC, lattice oxygen from the sample was emitted. Thus a series of complex reaction steps occurred on the surface of La_2CuO_4 over the temperature range where it is most sensitive to NO_2.

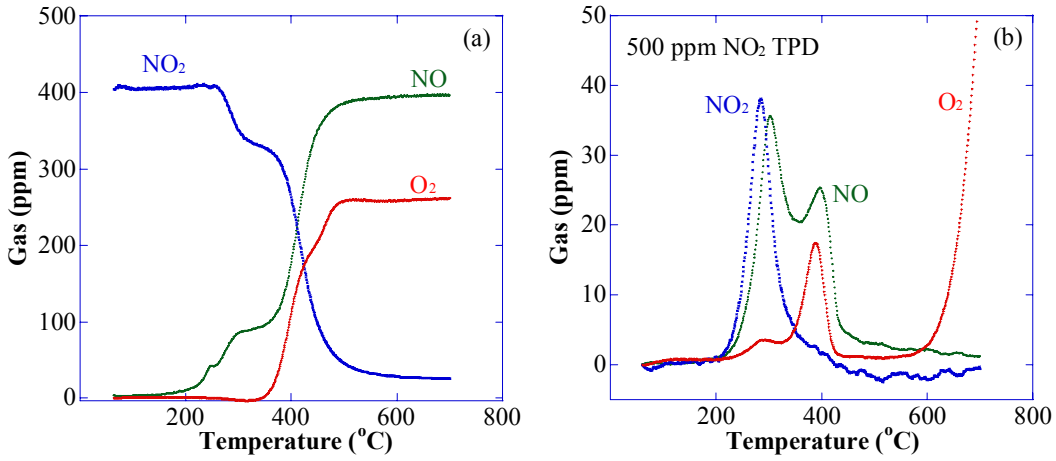

Fig. 7. TPR/TPD of NO_2 over the La_2CuO_4 powder. (a) TPR, (b) TPD of NO_2 (500 ppm).

4-1-3. Selectivity to NO

The response of the sensor with variation of NO concentration was studied in the presence of other gases. The NO sensitivity was not affected by the change of O_2 concentration (Fig. 8 (a)). In the NO+O_2 TPD experiments the NO adsorption was found to not be affected by O_2, showing NO desorption peaks very similar to those obtained in the NO TPD (Fig. 6 (a)).

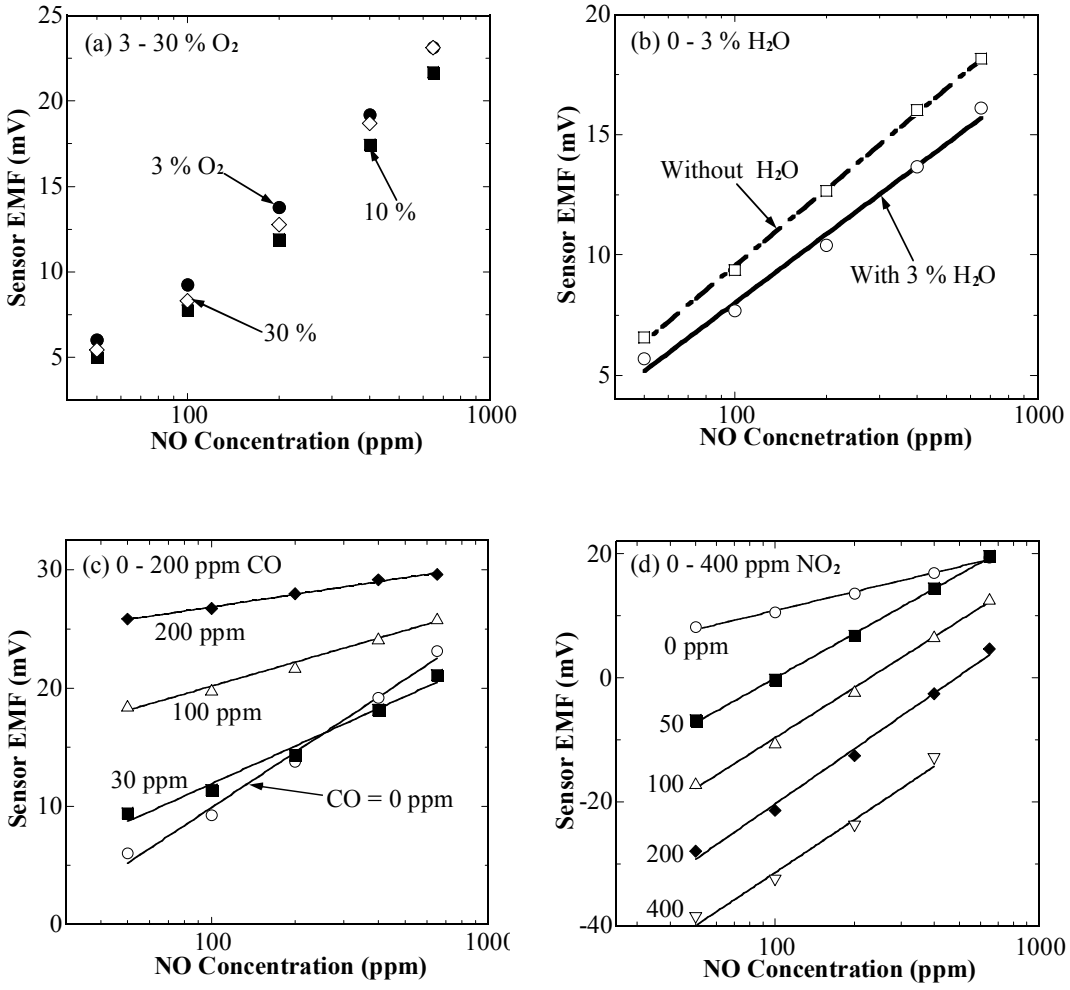

Fig. 8. Effect of O_2, H_2O, CO, NO_2, and CO_2 on the NO response at 450 ºC and in N_2. (a) O_2 effect (3 – 30 %), (b) H_2O effect (0 – 3 %), (c) CO effect (0 – 200 ppm), (d) NO_2 effect (0 – 400 ppm), (e) CO_2 effect (0 – 16 %). Measured in 3 % O_2 for (b) – (e).

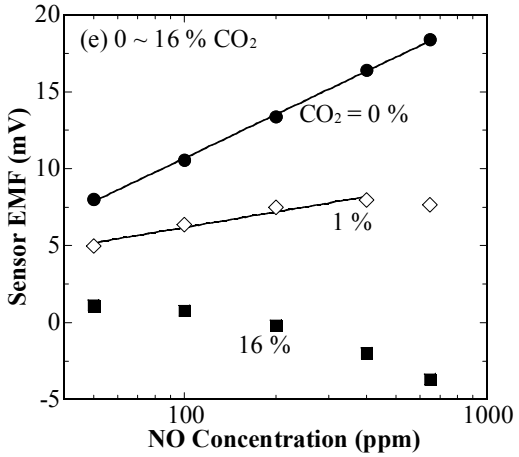

Fig. 8. (cont.) Effect of O_2, H_2O, CO, NO_2, and CO_2 on the NO response at 450 ºC and in N_2. (a) O_2 effect (3 – 30 %), (b) H_2O effect (0 – 3 %), (c) CO effect (0 – 200 ppm), (d) NO_2 effect (0 – 400 ppm), (e) CO_2 effect (0 – 16 %). Measured in 3 % O_2 for (b) – (e).

By addition of 3 % H_2O the sensor emf was reduced ~ 2 mV but the slope remained about the same (Fig. 8 (b)). The formation of a hydroxylated surface by water may influence the NO sensing behavior.

CO decreased the slope gradually and increased the emf values (Fig. 8 (c)). This is surprising since the response of the sensor to both NO and CO is positive. Thus one would expect an additive response. We find in Fig. 9 (a) that the presence of CO enhances NO adsorption so that NO continues to desorb up to 800 ºC (Compare Fig. 9 (a) to Fig. 6). Thus, the decrease in sensitivity with CO addition can be described in terms of the surface saturation that was exhibited for the NO response alone below 400 ºC (Fig. 5 (a)). The intense CO_2 desorption peak at 200 – 500 ºC in the NO+CO+O_2 TPD, probably formed by the surface reactions of CO with adsorbed oxygen or lattice oxygen. High CO oxidation catalytic activity was observed during the NO+CO+O_2 TPR above 200 ºC (Fig. 9 (b)).

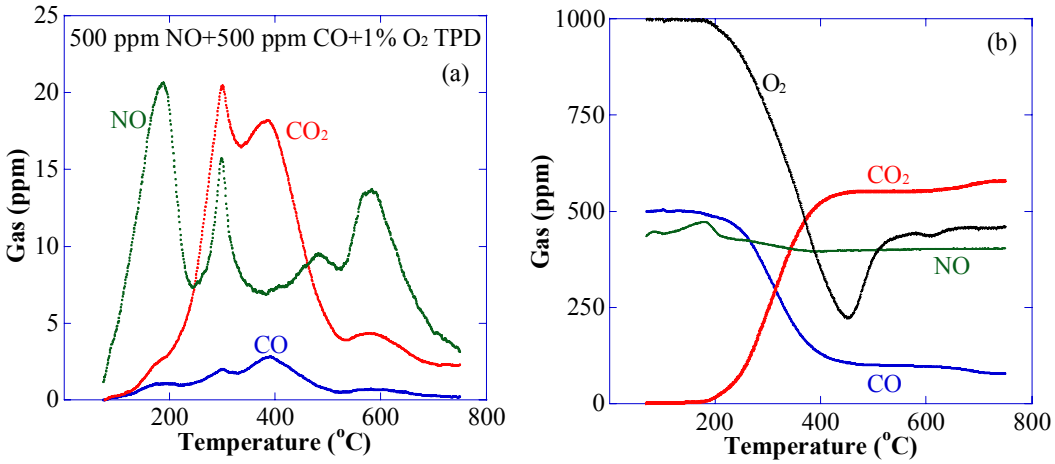

Fig. 9. TPD/TPR of NO+CO+O_2 over the La_2CuO_4 powder. (a) TPD of NO (500 ppm) + CO (500 ppm) + O_2 (1 %), (b) TPR.

Fig. 8 (d) showed that the NO sensitivity was strongly affected by NO_2, where the baseline shift occurred with the NO_2 concentration change. The slope remained positive even with the large changes in the emf values.

The effect of CO_2 is presented in Fig. 8 (e). High concentration of CO_2 reversed the NO sensitivity. This can be explained from the results of the NO+CO_2 TPD (Fig. 10). When NO and CO_2 were coadsorbed the CO_2 displaced the NO, shifting the NO desorption peaks to less than 200 ºC.

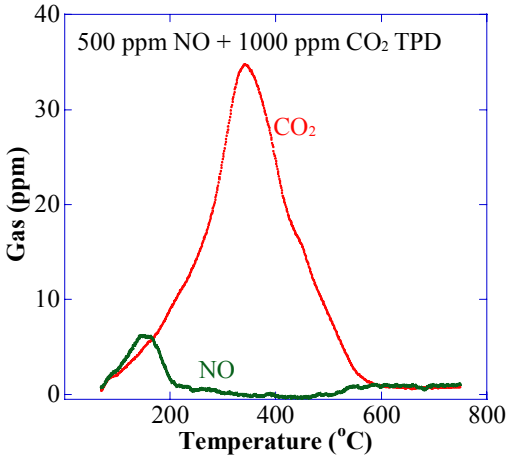

Fig. 10. TPD of NO (500 ppm) + CO_2 (1000 ppm) over the La_2CuO_4 powder.

4-2. WO_3-based Sensor

4-2-1. Characterization of WO_3 electrodes

Fig. 11 shows a scanning electron micrograph of a WO_3 and a Pt layer on the YSZ-8Y substrate prepared by sintering at 800 ^oC for 10 hr. The WO_3 thick film exhibited a very porous microstructure with 0.5 – 3 μm grains and 10 – 30 μm thickness. The porous Pt layer was deposited uniformly, showing a thickness ~ 9 μm.

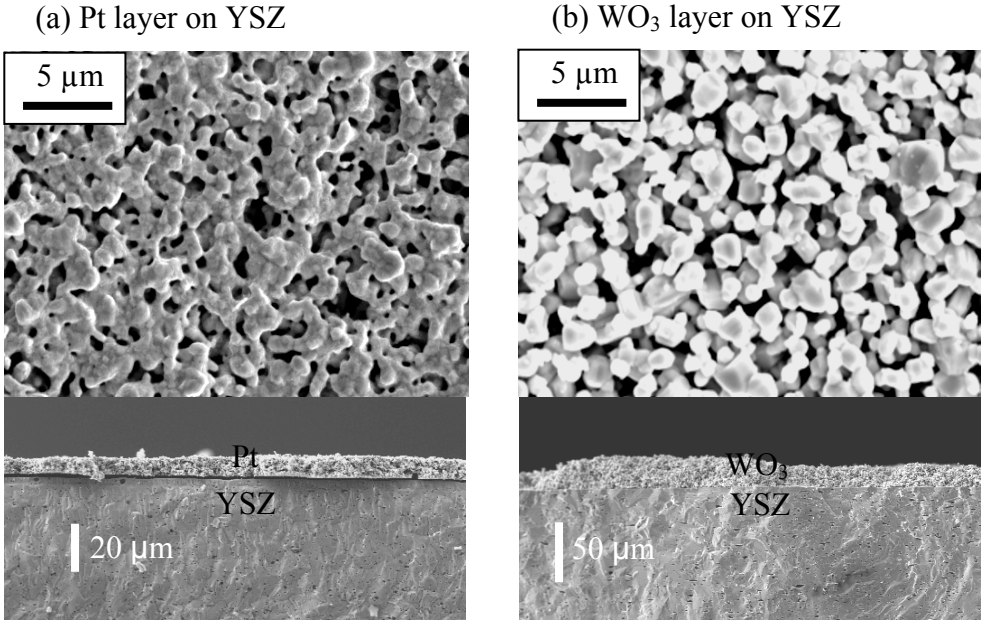

Fig. 11. Scanning electron micrograph of the Pt (a) and WO_3 (b) electrode.

4-2-2. Sensing properties

The sensor emf is plotted against time with NO concentration steps (50 – 650 ppm) and NO_2 steps (10 – 200 ppm) at 650 ^oC in 3 % O_2 (Fig. 12). A positive response was obtained for NO_2 and negative for NO. The direction of response of n-type semiconducting WO_3 is opposite to that of p-type La_2CuO_4. It agrees with the previous results, where the potentiometric sensor measurements were performed with different cell configurations [12, 13].

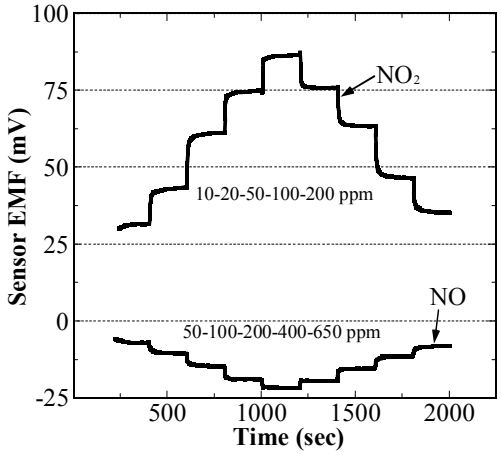

Fig. 12. Typical plot of sensor emf (mV) vs. time (sec) as a function of NO (50 – 650 ppm) and NO_2 (10 – 200 ppm) concentration steps at 650 ºC in 3 % O_2 and balance N_2.

Values of the emf measured for NO_2 were much higher than those formerly reported at 650 ^oC and in air. For example, value of the emf measured for 200 ppm NO_2 was ≈ 90 mV in the present experiments which is more than two times higher than in previous results [12, 13].

The response time (t_R) was dependent on the gas concentration, showing shorter t_R at higher concentration for both gases. The t_R was ≈ 20 sec for 400 – 650 ppm NO, and ≈ 50 sec for 50 – 100 ppm NO. The sensor response to 10 – 200 ppm NO_2 was faster than to NO with t_R less than 15 sec and attained a steady-state value within 60 sec at 650 ^oC even in the low concentration region, 10 – 20 ppm.

Measured emf values while increasing the NO_x concentration were slightly different from those in the regime of decreasing concentration at 650 ^oC. The difference of the emf values was ~ 3 mV at $NO_2 < 20$ ppm but less than 1 mV at $NO_2 > 100$ ppm, and less than 1 mV at $50 < NO < 400$ ppm. The difference decreased with increasing temperature and became negligible at T > 700 ^oC for both NO and NO_2, indicating that the kinetics of adsorption and desorption might be dissimilar at lower temperature. An average of the emf values measured with increasing and decreasing concentration was used for further analysis.

The measurements were repeated several times over 200 hr. Values of the emf obtained with the conditions described above were repeatable with less than 10 % difference. No systematic trend with the time sequence of the measurements was observed. However, the measurements were slightly affected by reducing (or oxidizing) gases exposure in the previous run and might cause the data scattering. Either changes in oxygen non-stoichiometry at the interfacial region caused by reducing or oxidizing gases or irreversible reactions of a gas with the surface layer most likely occurred.

Three different sensors of the same design were built and their sensing properties were compared with one another. The emf values measured for NO_x agreed within 15 % difference on average, under the same conditions. Properties of each sensor were expected to be slightly different because parameters affecting the sensitivity, such as porosity and thickness of electrode, might vary with fabrication process [14]. The differences are indicative of the importance of accurate control of fabrication conditions.

4-2-3. Temperature dependence of WO_3-based sensor

The temperature dependence of the NO_x emf response was investigated at $550 < T < 800$ °C (Fig. 13).

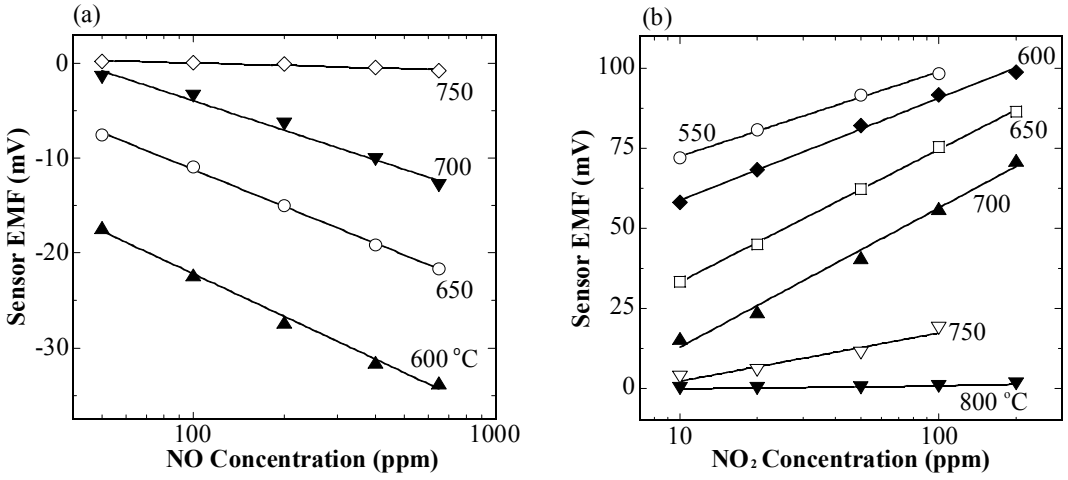

Fig. 13. Variation of the NO_x sensitivity as a function of temperature in 3 % O_2. (a) NO at 600 – 750 ºC, (b) NO_2 at 550 – 800 ºC.

A plot of the sensor emf (mV) vs. logarithm of NO concentration (ppm) is linear at 600 < T < 750 ^{o}C and 50 < NO < 650 ppm (Fig. 13 (a)). The slope decreased gradually with increasing temperature from 600 to 700 ^{o}C and decreased abruptly at 750 ^{o}C. The general tendency of the temperature dependence was in agreement with previous results obtained by using a half-open YSZ tube [12].

The temperature dependence of NO_2 sensitivity was also studied. As presented in Fig. 13 (b), a linear relationship was observed at 550 < T < 800 ^{o}C and 10 < NO_2 < 200 ppm. The slope increased slightly with temperature at 550 < T < 700 ^{o}C and a sudden decrease occurred at T > 750 ^{o}C, which was somewhat different from the previous observation showing an abrupt decrease in the slope at 700 ^{o}C [12].

As found for the WO_3-based sensor (Fig. 13), the sensor response decreases with increasing operating temperature [15, 16]. This is due in part to the amount of adsorbed gas on the surface of the semiconductor which decreases with temperature, as the rate of gas desorption is faster than that of adsorption [5]. In addition, a dissymmetry of the catalytic activity between the two electrodes could also explain it. TPR experiments of the catalytic activity of a Pt electrode for the reduction of NO_2 was found to be higher than that of WO_3 (Fig. 14). With increasing temperature the difference in the activity became smaller, reducing the sensor response.

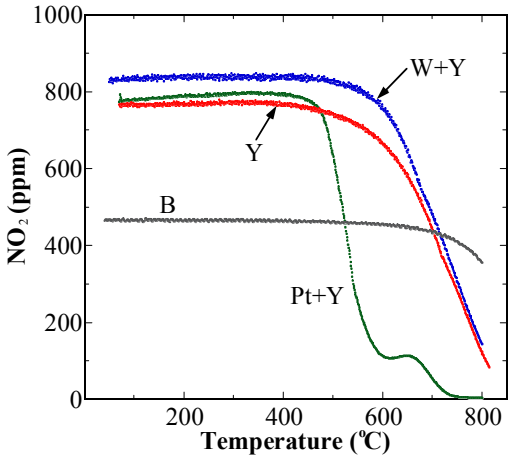

Fig. 14. TPR of NO_2 over WO_3 on YSZ (W+Y), Pt on YSZ (Pt+Y), YSZ (Y), and blank (B).

4-2-4. Selectivity to NO

The effect of H_2O, NO_2, CO, CO_2, and O_2 on the NO sensitivity was investigated at 650 ^oC. Fig. 15 shows plots of the sensor response to NO in the existence of other gases.

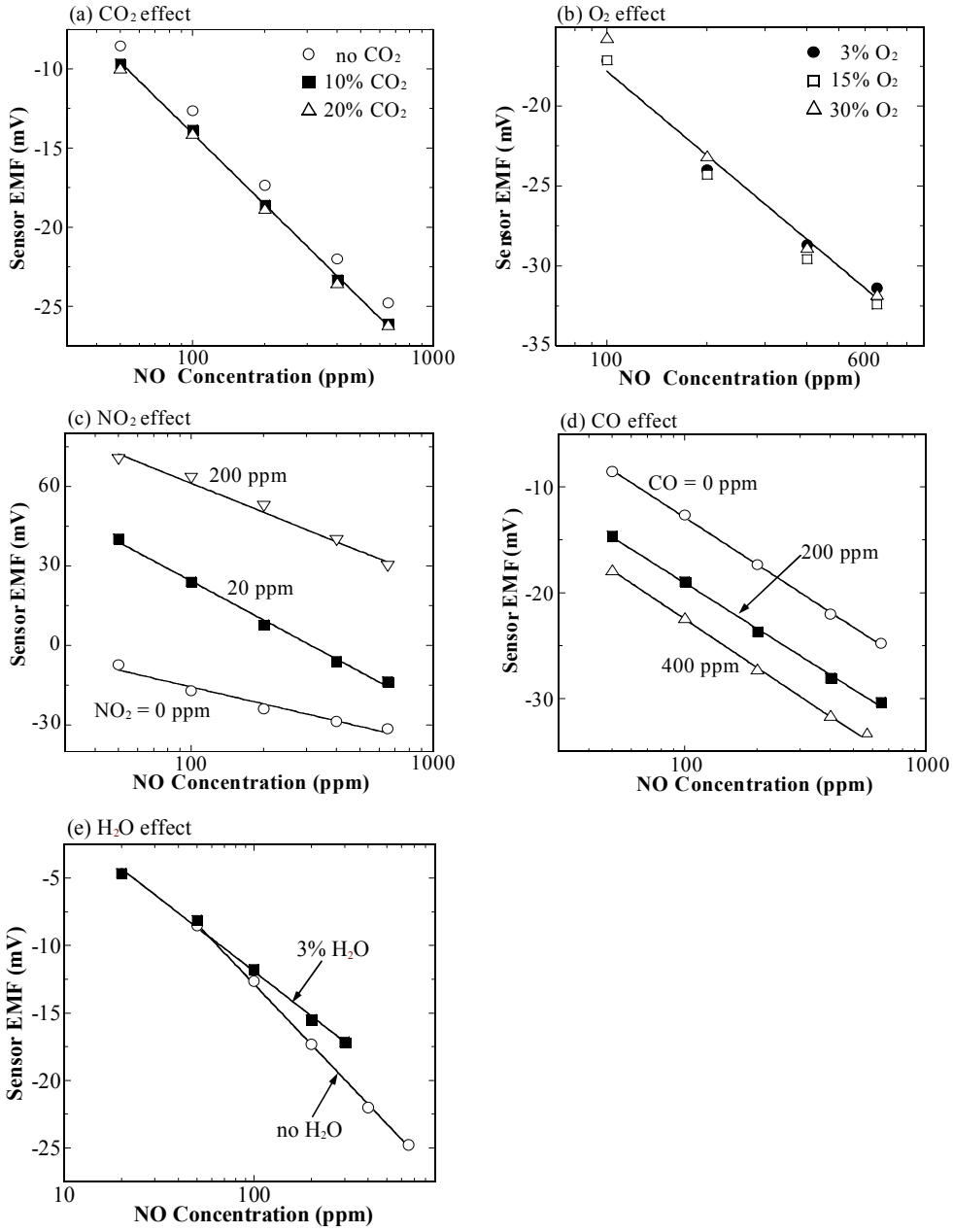

Fig. 15. Effect of CO_2, O_2, NO_2, CO, and H_2O on the NO response at 650 ºC and in N_2 balance. (a) CO_2 effect (0 – 20 %), (b) O_2 effect (3 – 30 %), (c) NO_2 effect (0 – 200 ppm), (d) CO effect (0 – 400 ppm), (e) H_2O effect (0 – 3 %). Measured in 3 % O_2 for (a) and (c) – (e).

The WO_3-based sensor was able to selectively detect NO in the presence of CO_2 (Fig. 15 (a)). Values of the sensor emf with three different concentrations of CO_2 were very close to each other, exhibiting a maximum difference of emf values less than 1.5 mV. The sensor was also selective to NO without any interference by changing O_2 concentration, 3 – 30 % (Fig. 15 (b)).

The influence of NO_2 on the NO sensitivity is shown in Fig. 15 (c). When NO_2 was added to the NO step, values of the emf increased significantly but the sign of the slope was not changed. The slope increased considerably by the addition of 20 ppm NO_2. The gas-phase oxidation of NO, eqn. (1), is thermodynamically favorable in the present condition and thus in equilibrium most of the NO should be converted to NO_2.

$$NO + 1/2O_2 \rightarrow NO_2 \quad (1)$$

However, no conversion of NO to NO_2 was observed in the TPR experiments (Fig. 16), because of unfavorable NO oxidation kinetics. As discussed previously for the La_2CuO_4-based sensor, the mixed potential theory cannot explain the occurrence of the NO sensitivity of the WO_3-based sensor.

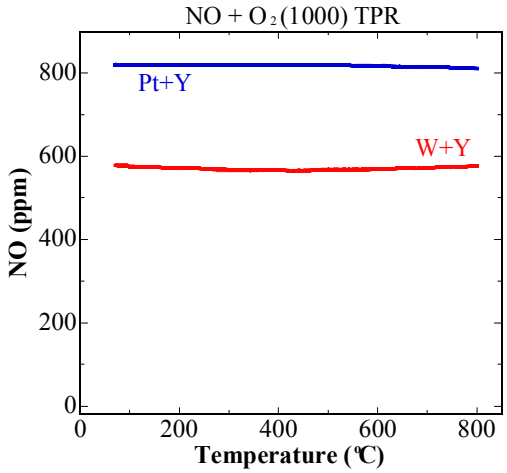

Fig. 16. TPR of $NO+O_2$ (1000 ppm) over WO_3 on YSZ (W+Y) and Pt on YSZ (Pt+Y).

Fig. 15 (d) shows the effect of CO on the NO sensor response. Values of the emf increased without significant change of slope. In the TPR experiments (Fig. 17) WO_3 and

Pt electrodes exhibited different catalytic activities for the oxidation of CO at 650 °C, either non-electrochemically (eqn. (2)) or electrochemically (eqn. (3)).

$$CO + 1/2O_2 \rightarrow CO_2 \quad (2)$$

$$CO + O^{2-}_{(lattice)} \rightarrow CO_2 + 2e^- \quad (3)$$

This difference might give rise to the CO response. However, neither CO_2 formation from the reaction of NO with CO, eqn. (4), nor the oxidation of NO, eqn. (1), was observed in the present system.

$$CO + NO \rightarrow CO_2 + 1/2N_2 \quad (4)$$

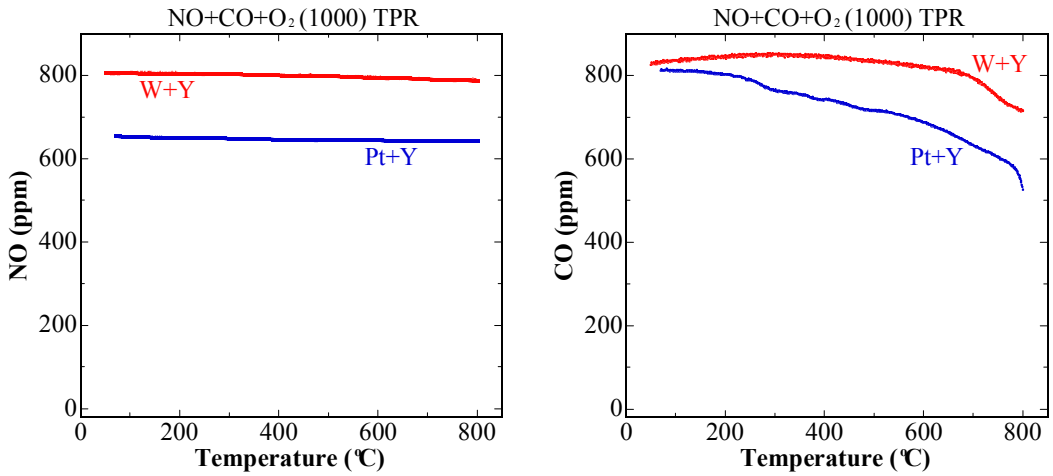

Fig. 17. TPR of NO+CO+O_2 (1000 ppm) over WO_3 on YSZ (W+Y) and Pt on YSZ (Pt+Y).

Water is known to be strongly adsorbed on the surface of metal oxides, giving a so called hydroxylated surface, where the OH^- anions are bonded to the metal cations, and the H^+ ion to the oxide anions [5]. As shown in Fig. 15 (e), the slope decreased slightly by addition of 3 % H_2O. A linear relationship was still shown even in the presence of H_2O.

4-2-5. Selectivity to NO_2

The influence of CO_2 (0 – 20 %) and H_2O (0 – 3 %) on the NO_2 response at 650 ^oC is presented in Fig. 18 (a) and (b), respectively. The difference in emf values with and without CO_2 and H_2O was less than 1 mV in the whole NO_2 concentration range.

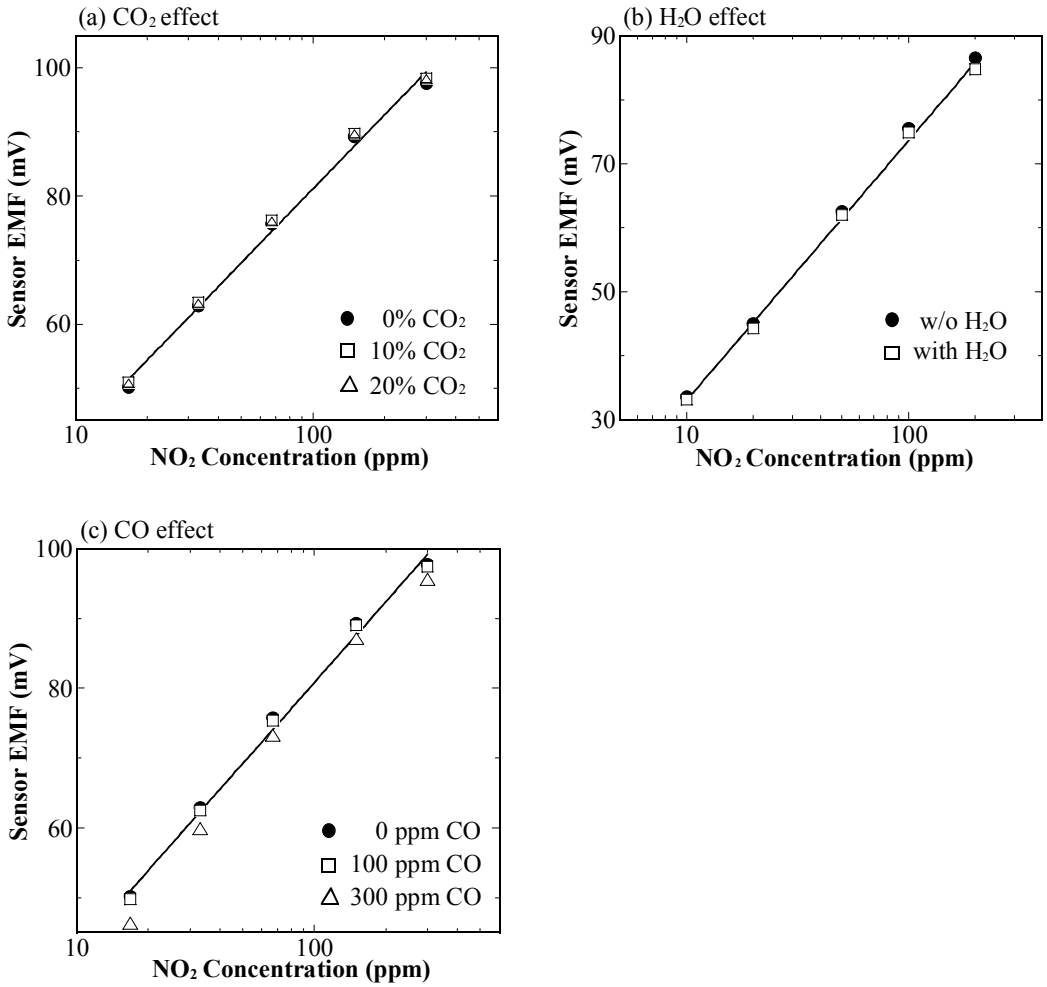

Fig. 18. Effect of CO_2, H_2O, and CO on the NO_2 response at 650 ºC in 3 % O_2. (a) CO_2 effect (0 – 20 %), (b) H_2O effect (0 – 3 %), (c) CO effect (0 – 300 ppm).

As shown in Fig. 18 (c), the addition of 100 and 300 ppm CO did not influence the NO_2 sensitivity. Values of the emf obtained with 300 ppm CO were ~ 3 mV smaller than those without CO, but the difference was still within the general range of reproducibility. As

commented previously, the selective detection of NO against NO_2 and CO was not accomplished, but interestingly the NO_2 response was not influenced by CO. In the NO_2+CO+O_2 TPR experiments (Fig. 19) the NO_2 reduction reactions, eqn. (5) and (6), were found to be dominant at 650 ºC over the CO oxidation reactions, eqn. (2) and (3), and that was likely why the influence of CO was not significant.

$$NO_2 \rightarrow NO + 1/2O_2 \quad (5)$$

$$NO_2 + 2e^- \rightarrow NO + O^{2-}_{(lattice)} \quad (6)$$

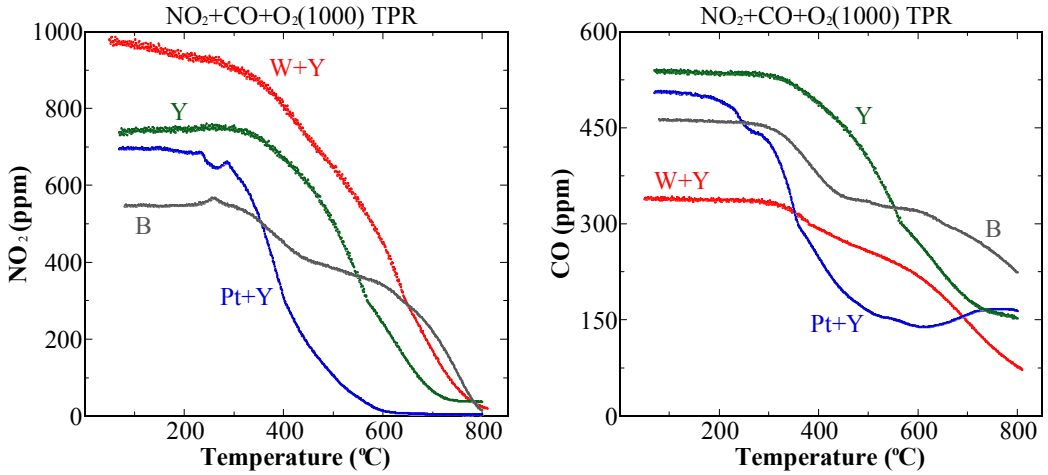

Fig. 19. TPR of NO_2+CO+O_2 (1000 ppm) over WO_3 on YSZ (W+Y), Pt on YSZ (Pt+Y), YSZ (Y), and blank (B).

The present sensor made of YSZ-8Y with a Pt and a WO_3 electrode is very promising for the monitoring of NO_2, as it selectively detected NO_2 with very high sensitivity down to low concentrations NO_2 (~ 10 ppm).

4-2-6. Sensing properties of WO_3 based sensor in simulated exhaust

Comparison of the NO_x response between the sensor in 3 % O_2 and the sensor in simulated exhaust condition (3 % O_2, 3 % H_2O, 16 % CO_2, and 100 ppm CO) is given at 650 ^oC and 10 < NO_x < 650 ppm (Fig. 20).

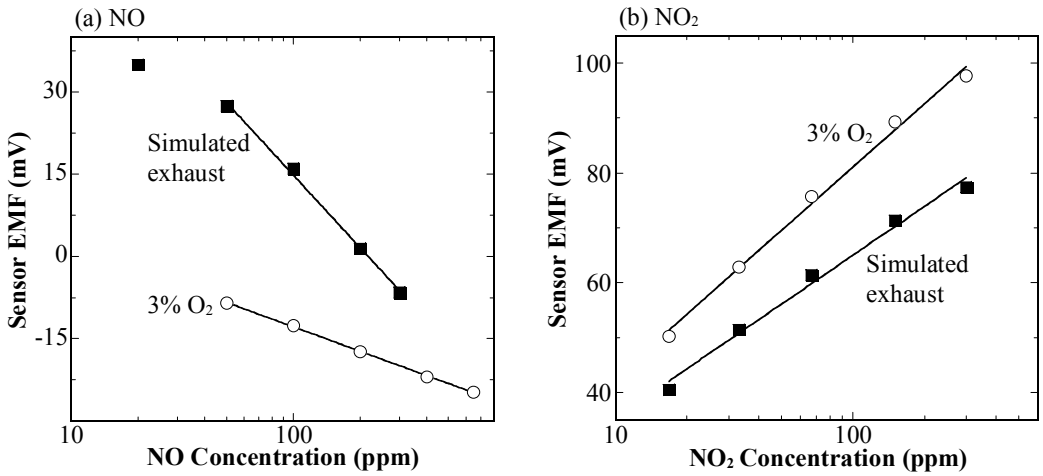

Fig. 20. Comparison of the NO_x sensitivity at 650 ºC between in 3 % O_2 and in a simulated exhaust gas (3 % O_2, 3 % H_2O, 16 % CO_2, and 100 ppm CO). (a) NO, (b) NO_2.

The exhaust condition included most gases generally formed during the combustion process, except hydrocarbons. Values of the emf measured for NO were significantly different for each condition and the slope of the plot was much greater in the exhaust gas than in 3 % O_2 (Fig. 20 (a)). This higher sensitivity for NO in combustion gas than in 3 % O_2/N_2 mixture indicates a complex equilibrium occurs on the electrode surface when all gas species are present. In contrast, Fig. 20 (b) shows that in the exhaust both values of the emf and the slope for the NO_2 step decreased compared to those in 3 % O_2.

The influence of each of the individual gases on the NO_x response was investigated and the results are shown in Fig. 21 and 22. For example, to study the effect of O_2, measurements were performed by varying O_2 concentration (0.5 – 20 %) while maintaining constant concentrations of the other gases (3 % H_2O, 16 % CO_2, and 100 ppm CO). Similarly, the effect of H_2O (0 – 3 %), CO_2 (0 – 16 %), and CO (0 – 200 ppm) was studied.

4-2-7. Selectivity to NO in simulated exhaust

As presented in Fig. 21 (a) ~ (d), the NO sensing behavior was strongly affected by H_2O, O_2, and CO, but not by CO_2.

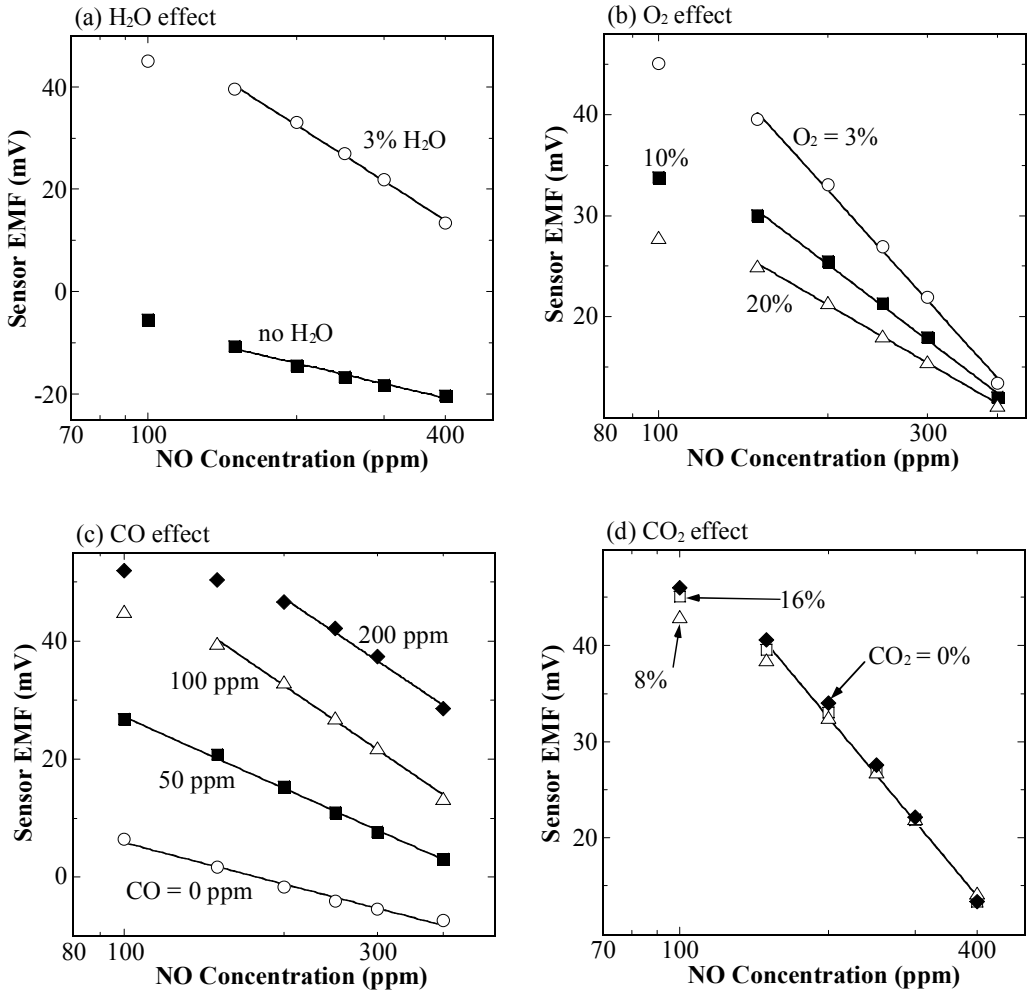

Fig. 21. Effect of H_2O, O_2, CO, and CO_2 on the NO response at 650 ºC and in a simulated exhaust gas (3 % O_2, 3 % H_2O, 16 % CO_2, and 100 ppm CO). (a) H_2O effect (0 – 3 %), (b) O_2 effect (3 – 20 %), (c) CO effect (0 – 200 ppm), (d) CO_2 effect (0 – 16 %).

The effect of H_2O in the combustion gas mixture was especially remarkable (Fig. 21 (a)). 3 % H_2O increased the emf by more than 40 mV at the same NO concentration. Further, the

NO sensitivity increased in the combustion mixture, whereas it decreased in the simple N_2 based gas mixtures. As shown in Fig. 15 (e) the effect of 3 % H_2O on the NO response in 3 % O_2 was much smaller than in the gas mixture, indicating water vapor itself did not greatly affect sensitivity. Therefore, the large change in response by H_2O is probably due to the water vapor on the surface of the electrode enhancing the kinetics of NO_2 production (eqn. (1) and (7)) [5, 17] or the formation of complex NO–H_2O surface species.

$$NO + H_2O \rightarrow NO_2 + H_2 \quad (7)$$

Fig. 21 (b) shows the effect of O_2 on NO sensitivity. Increasing the concentration of O_2 caused both values of the sensor emf and the slope to decrease in contrast to the N_2 mixture where it was independent (Fig. 15 (b)). The influence of CO was also significant (Fig. 21 (c)). The slope of the NO step was enhanced by the addition of 50 – 200 ppm CO. Values of the emf increased with CO in the exhaust gas, which is opposite to the results obtained in 3 % O_2, where the emf value decreased with CO (Fig. 15 (d)). As the cross-sensitivity of O_2 is negligible in an N_2 environment and the cross-sensitivity of CO is much smaller than that of NO, the sensing behaviors with O_2 and CO are influenced by the complex equilibrium in the combustion gas mixture.

The NO response was not influenced by inert CO_2 gas (0 ~ 16 %) (Fig. 21 (d)).

4-2-8. Selectivity to NO_2 in simulated exhaust

The plots showing the effect of O_2 and H_2O at 650 ^oC on the NO_2 response are given in Fig. 22. Values of the emf for NO_2 were reduced with increasing O_2 concentration (Fig. 22 (a)). In the range of 3 – 20 % O_2 no clear change of the slopes was observed, but a small increase of the slope with 0.5 % O_2 was seen when compared to the response in 3 – 20 % O_2. The same explanation used in the previous section might be applicable. The addition of 3 % H_2O decreased the slope with reduced values of the emf (Fig. 22 (b)). Interestingly, the plot obtained without 3 % H_2O in simulated exhaust was very similar to that in 3 % O_2 (Fig. 20 (b)), showing H_2O played an important role in the NO_2 sensitivity. Both CO (0 – 200 ppm) and CO_2 (0 – 16 %) did not have a significant effect on the sensing of NO_2 (Fig. 22 (c) and (d)).

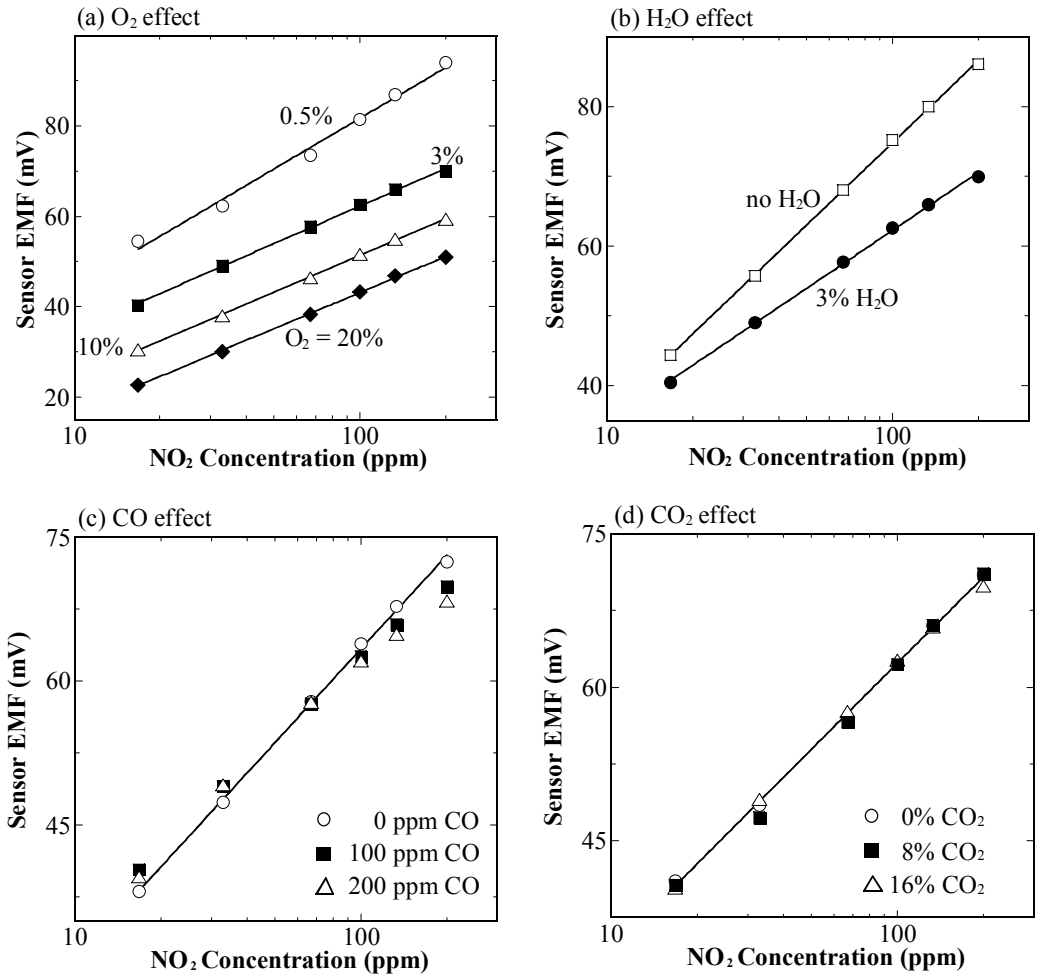

Fig. 22. Effect of O_2, H_2O, CO, and CO_2 on the NO_2 response at 650 ºC and in a simulated exhaust gas. (a) O_2 effect (0.5 – 20 %), (b) H_2O effect (0 – 3 %), (c) CO effect (0 – 200 ppm), (d) CO_2 effect (0 – 16 %).

5. CONCLUSION

The NO_x sensing properties were studied using a potentiometric sensor (Pt/YSZ/WO_3 or La_2CuO_4) with $0 < NO_x < 650$ ppm. For the WO_3-based sensor (n-type semiconductor) a positive response was shown for NO_2 but negative for NO at 650 ºC. In contrast for the p-type semiconducting La_2CuO_4-based one the opposite direction of the response for NO_x was observed at 450 ºC. A linear relationship was obtained in the plot of the emf vs. the logarithm of NO_x concentration for both.

With the WO_3-based sensor, H_2O and CO had an effect on the NO sensitivity but not on NO_2 sensitivity in 3 % O_2 environment, showing it can be used to detect ~ 10 ppm NO_2 selectively. Values of the emf measured with NO in simulated exhaust gas were considerably different from those in 3 % O_2. This difference indicated a possible gas composition change at 650 ºC and the formation of a hydroxylated surface by water. The NO_2 sensitivity also changed in simulated exhaust gas, but not as much.

The results obtained with the La_2CuO_4-based sensor seemed to indicate that the temperature was the only significant factor in the sensor response for NO in 3 % O_2, as the experiments above 400 ^oC showed good response time and the major tradeoff became sacrificing signal strength for stability. When comparisons were made to the NO TPD results, we found that the temperature dependence was consistent with our proposed "Differential Electrode Equilibria" mechanism. The NO_2 response was also strongly temperature-dependent with an abrupt decrease above 500 ^oC.

6. REFERENCES

1. T. Inoue, K. Ohtsuka, Y. Yoshida, Y. Matsuura, Y. Kajiyama, Metal oxide semiconductor NO_2 sensor, *Sensors and Actuators B*, **24-25**, (1995), 388-391.

2. Y. Wu, Z. Zhao, Y. Liu, X. Yang, The role of redox property of $La_{2-x}(Sr,Th)_xCuO_{4-\delta}$ playing in the reaction of NO decomposition and NO reduction by CO, *J. of Mol. Cat. A: Chemical*, **155**, (2000), 89-100.

3. H. Oshima, M. Tatemichi, T. Sawa, Chemical Basis of inflammation induced carcinogenesis, *Archives of Biochemistry and Biophysics*, **417**, (2003), 3-11.

4. F. Ménil, V. Coillard, C. Lucat, Critical review of nitrogen monoxide sensors for exhaust gases of lean burn engines, *Sensors and Actuators B*, **67**, (2000), 1-23.

5. M. J. Madou, S.R. Morrison, Chemical Sensing with solid state devices, Academic press. (1989).

6. E. D. Wachsman and P. Jayaweera, Solid State Ionic Devices II - Ceramic Sensors, The Electrochem. Soc. Proceedings 2001, E.D. Wachsman, W. Weppner, E. Traversa, M. Liu, P. Vanysek, and N. Yamazoe, Ed., **2000-32**, 298-304.

7. E. Di Bartolomeo, M.L. Grilli, and E. Traversa, Solid State Ionic Devices III, The Electrochem. Soc. Proceedings 2003, E. D. Wachsman, K. Swider-Lyons, M. F. Carolan, F. H. Garzon, M. Liu, and J. R. Stetter, Ed. **2002-26**, 222-235.

8. E.D. Wachsman, Solid-State Ionic Devices III, The Electrochem. Soc. Proceedings, 2003, E. D. Wachsman, K. Swider-Lyons, M. F. Carolan, F. H. Garzon, M. Liu, and J. R. Stetter, Ed., **2002-26**, 215-221.

9. E. Di Bartolomeo, N. Kaabbuathong, M.L. Grilli, E. Traversa, Planar electrochemical sensors based on tape-cast YSZ layers and oxide electrodes, *Solid State Ionics*, **171**, (2004), 173-181.

10. E. Traversa, A. Bearzotti, M. Miyayama, H. Yanagita, Influence of the Electrode Materials on the Electrical Response of ZnO-based Contact Sensors, *J. of the European Ceramic Society*, **18**, (1998), 621-631.

11. N. Miura, T. Raisen, G. Lu, and N. Yamazoe, Highly selective CO sensor using stabilized zirconia and a couple of oxide electrodes, *Sensors and Actuators B*, **47**, (1998), 84-91.

12. G. Lu, N. Miura, & N. Yamazoe, Stabilized zirconia-based sensors using WO_3 electrode for detection of NO or NO_2, *Sensors and Actuators B*, **65**, (2000), 125-127.

13. A. Dutta, N. Kaabbuathong, M. L. Grilli, E. Di Bartolomeo, and E. Traversa, Study of YSZ-based electrochemical sensors with WO_3 electrodes in NO_2 and CO environments, *J. Electrochem. Soc.*, **150**, (2003), H33-H37.

14. H. T. Sun, C. Cantalini, L. Lozzi, M. Passacantando, S. Santucci, and M. Pelino, Microstructural effect on NO_2 sensitivity of WO_3 thin film gas sensors, *Thin Solid Films*, **287**, (1996), 258-265.

15. S. Zhuiykov, M. Muta, T. Ono, M. Hasei, N. Yamazoe, and N. Miura, Stabilized zirconia-based NO_x sensor using $ZnFe_2O_4$ sensing electrode, *Electrochemical and solid-state letters*, **4**, (2001), H19-H21.

16. G. Lu, N. Miura, and N. Yamazoe, Mixed potential hydrogen sensor combining oxide ion conductor with oxide electrode, *J. Electrochem. Soc.*, **143**, (1996), L154-L155.

17. N. Sakai, K. Yamaji, T. Horita, H. Kishmoto, Y. P. Xiong, and H. Yokokawa, Significant effect of water on surface reaction and related electrochemical properties of mixed conducting oxides. *Solid State Ionics*, **175**, (2004), 387-391.